Journal of Optoelectronics and Advanced Materials Vol. 5, No. 5, 2003, p. 1439 - 1443

MULTICOMPONENT DIFFUSION AND REACTION IN THREE-DIMENSIONAL NETWORKS

V. Popescu, C. Oprea[a*], S. Birghila

Department of Chemistry, Ovidius University, Constanta, Romania
[a]Department of Physics, Ovidius University, Constanta, Romania

Due to the complicate interaction of diffusion and reaction in catalysts more detailed models of porous structures are needed. We have based our model on a three-dimensional network of interconnected cylindrical pores as pore model, although the treatment is applicable to alternative pore geometries. The network assumed has predefined distributions of pore radii, connectivity and porosity. Mass transport in the individual pores of the network is described by the dusty-gas model. In contrast to previous publications, the present network model can be applied to any common reaction kinetics. This becomes quite inevitable in order to make three-dimensional network models applicable to practical problems in industry. To solve the mass balances within the entire network, the mass balances for individual pores have to be solved simultaneously, since these mass balances are coupled by the boundary conditions at the nodes of the network. The system of differential equations has been solved by the finite-difference method. To solve the resulting large nonlinear system, a Schur complement method was used.

(Received July 15, 2003; accepted August 28, 2003)

Keywords: Fractal geometry, ZSM-5 zeolite, Kinetic parameters, Electronic microscopy

1. Introduction

Porous catalyst supports are in widespread use in the chemical industry. Reactants diffuse into the void space of the support, react, and products formed diffuse out of the pellet. Multicomponent diffusion within the catalyst supports, which have a very complicated geometrical structure, has to be described. Molecular diffusion, Knudsen and surface diffusion can all occur. On fractal surfaces anomalous diffusion will take place, [1], and in microporous materials, configurational diffusion may be the dominating mass transport mechanism. A quite useful approximation based on Boltzmann's equations, the dusty-gas model, has been developed (Mason and Malinauskas, [2]). This model describes the molecular diffusion, Knudsen diffusion, viscous flux, and in principle, the surface diffusion, with sufficient accuracy.

The fundamentals underlying surface diffusion, configurational and anomalous diffusion are still under investigation. Molecular dynamics and Monte Carlo approaches are the preferred methods of calculation for these transport mechanisms. Following the attempts of Wakao and Smith (1962), Johnson and Stewart (1965) and Foster and Butt (1966) to describe the porous structure of catalyst pellets, capillary Bethe lattices and random networks were employed to model the structure of porous materials. Reyes and Jensen (1985), Beeckman et al. (1978) and Beeckman and Froment (1980), [3], have also used a Bethe lattice representation of the porous medium. In this model no closed loops and a fixed connectivity are employed. Gavalas and Kim (1981), [4], and Petropoulos et al. (1991), [5], have introduced capillary networks whereas Sharratt and Mann (1987), [6], have studied the properties of random networks.

Recent applications of network models are presented by Arbabi and Sahimi (1991), [7], Sahimi (1992), [8], McGreavy (1992), [9], Zhang and Seaton (1992), [10], amongst others. Keil and

* Corresponding author: coprea@univ-ovidius.ro

Rieckman (1994), [11] have optimized catalyst pore structures for the hydro-demetallation process with the aid of three-dimensional lattice models.

2. Model

The catalytic active crystallites are distributed within the pore space of a support. The reactants have to diffuse into the pore space, where they react at the active centers to form products. The type of diffusion (Knudsen diffusion, bulk or molecular diffusion, configurational diffusion, surface diffusion, anomalous diffusion) depends on the size of the pores, the molecules involved, the operating conditions and the surface geometry of the pores.

As the pore network is composed of single cylindrical pores of different diameters, the dusty-gas model for a single pore was used as a starting point. The dusty-gas model combines the contributions of Knudsen and molecular fluxes.

Solution of the model equations

For each individual pore one has to solve a boundary value problem. The boundary conditions of different pores are coupled by Kirchhoff's Law. The boundary value problems of the pores have to be solved simultaneously. The model equations were solved by the finite-difference method.

Each pore was discretized in axial direction (Fig. 1).

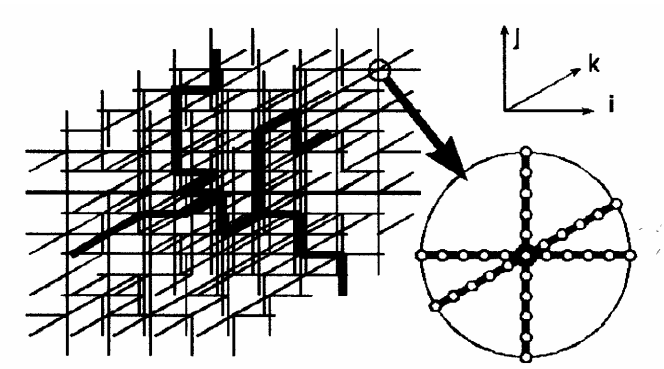

Fig. 1. Discetization of the pore network.

Derivatives were approximated by finite-difference formulae. At interior points of the pores, the following central difference formulae were used:

$$\frac{dc}{dw} = \frac{c_{k+1} - c_{k-1}}{2\Delta w} + O(\Delta w^2)$$

$$\frac{d^2c}{dw^2} = \frac{c_{k+1} - 2c_k + c_{k-1}}{\Delta w^2} + O\left(\Delta w^2\right)$$

At the pore ends, one-sided difference formulae were employed:

$$\left.\frac{dc}{dw}\right|_{w=0} = \frac{-3c_0 + 4c_1 - c_2}{2\Delta w} + O\left(\Delta w^2\right)$$

$$\left.\frac{dc}{dw}\right|_{w=L_p} = \frac{c_{n-2} - 4c_{n-1} + 3c_n}{2\Delta w} + O\left(\Delta w^2\right) \ .$$

Introducing these difference formulae into the equations for each pore, each inner node and each outer node of the network leads to a large system of nonlinear equations: F(c) =0.

The structure of the Jacobian matrix is shown in Fig. 2.

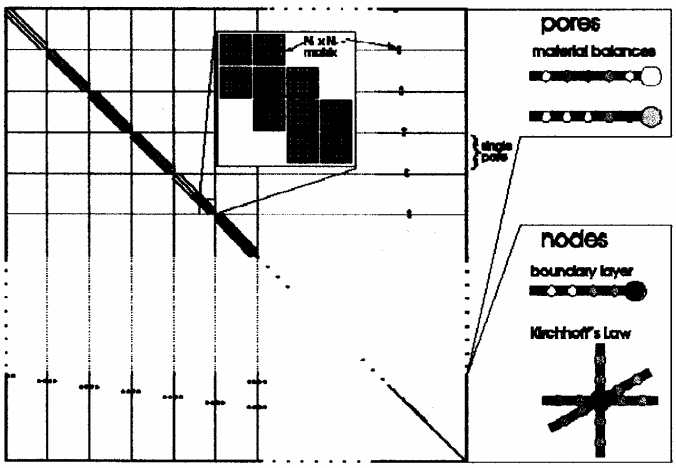

Fig. 2. Structure of the Jacobian matrix.

The equations for the pores are located in the upper part of the matrix, those for the nodes in the lower part. The entries for the concentrations within the pores are to be found on the left hand side, the concentrations at the nodes on the right hand side.

Due to the central difference formulae the material balances inside the single pores lead to a tridiagonal band of $N_k \times N_k$-matrices. At the ends of each pore the equations are coupled with the concentrations at the nodes.

The equations for the nodes lead to a diagonal band of $N_k \times N_k$-matrices. For each of the pores entering a node there are two entries in the form of $N_k \times N_k$-matrices, because of the one-sided difference formulae at the pore ends.

The matrix is nonsymmetrical and not diagonally dominant. This makes the solution of the present nonlinear system of equations difficult. The eigenvalues of the matrix range from -1.9×10^5 to $+1.8\times10^{-2}$.

3. Results and discussion

The algorithm can be adapted to any common form of reaction kinetics, which makes it applicable to industrial problems. Using the algorithm described in the previous paragraphs one has to provide the following experimental data:

- rate expressions of the intrinsic kinetics;
- distribution of pore radii and void fractions, taken from BET or mercury porosity measurements;
- connectivity found by the method presented by e.g. Seaton (1991), [12], from BET measurements;
- binary transport parameters (may also be calculated if not available).

As an example we have used the reaction kinetics of a coking reaction of a reaction scheme described by Beyne and Froment (1993), [13], suitable for modeling the deactivation of a ZSM-5 catalyst due to coke formation. The coke formation starts with the deposition of a coke precursor, proceeds through growth reactions and stops under the influence of termination reactions. Both parallel and consecutive coking mechanisms were considered. The kinetic equations are of the Hougen-Watson type.

Three stages in the coke formation process were distinguished:

a. formation of coke precursor, C_p, from one or more reaction components;
b. coke growth: conversion of coke precursor into a growing species, C_g;
c. termination of the coke growth: formation of a nonreactive coke, C_t.

The detailed mechanism of these three steps is shown in next table.

Reaction scheme and adsorption and reaction rate constants Step constant	Data used for the simulations
$A + l \Leftrightarrow Al\ K_A$ $Al \Rightarrow Bl\ k_{AB}$ $Bl \Leftrightarrow B + l\ K_B$ $Al \Rightarrow C_p\ k_{iB}$ $C_p + A \Rightarrow C_g\ k_{gA}$ $C_p + B \Rightarrow C_g\ k_{gB}$ $C_g + A \Rightarrow C_g\ k_{gA}$ $C_g + B \Rightarrow C_g\ k_{gB}$ $C_g + A \Rightarrow C_t\ k_{tA}$ $C_g + B \Rightarrow C_t\ k_{tB}$	$r_m = 2.10^{-8}$ m ; $r_M = 1.5\times10^{-7}$ m $e_m = 0.124$; $e_M = 0.05$ $s_m = 0.2$; $s_M = 0.2$ $d_p = 5.10^{-3}$ m $D_A = D_B\ 10^{-5}\ m^2s^{-1}$ $Z = 4$; $b = 1\ ms^{-1}$ $K_A = K_B\ 0.49\ m^3mol^{-1}$ $MW_A = MW_B\ 86\ gmol^{-1}$ $r_C = 1800\ kgm^{-3}$ $C_t = 10^{-6}\ molm^{-2}$ $K_{AB} = 0.175\ ls^{-1}$ $K_{iA} = K_{iB}\ 10^{-4}\ ls^{-1}$ $k_{gA} = k_{gB}\ 7.3\times10^{-6}\ m^3/(mol.s)$ $k_{tA} = k_{tB}\ 7.3\times10^{-6}\ m^3/(mol.s)$ T = 800 K

The following reaction rate expressions correspond to the reaction steps of table:

$$v_{AB} = \frac{k_{AB}K_AC_tC_A}{1+K_AC_A+K_BC_B}\left(1-\frac{C_{Cl,acc}}{C_t}\right)$$

$$v_{iA} = \frac{k_{iA}K_AC_tC_A}{1+K_AC_A+K_BC_B}\left(1-\frac{C_{Cl,acc}}{C_t}\right)$$

$$v_{iB} = \frac{k_{iB}K_BC_tC_B}{1+K_AC_A+K_BC_B}\left(1-\frac{C_{Cl,acc}}{C_t}\right)$$

$$v_{pgA} = k_{gA}C_{Cp,acc}C_A$$
$$v_{pgB} = k_{gB}C_{Cp,acc}C_B$$
$$v_{gA} = k_{gA}C_{Cg,acc}C_A$$
$$v_{gB} = k_{gB}C_{Cg,acc}C_B$$
$$v_{tA} = k_{tA}C_{Cg,acc}C_A$$
$$v_{tB} = k_{tB}C_{Cg,acc}C_B$$

The catalyst data and the kinetic parameters listed in table have been used for the simulations. A micro porous network augmented with a macro porous network was used. The micro- and macropore radii had a Gaussian distribution function with predescribed mean values r_m and r_M and predescribed standard deviations s_m and s_M.

Different boundary conditions were assumed for the outer surfaces of the network. One surface was assumed to be in contact with the bulk phase, the other five surfaces to be closed with symmetry conditions pertaining (see a two dimensional section in Fig. 3).

The reaction mechanism consists of parallel coking reaction steps where in which coke is formed from the component A, and consecutive coking reactions steps where coke is formed the component B. The concentrations and coke deposition profiles were calculated for the case of consecutive coking. A network of 10×10×10 nodes has been used for the calculations. The network was generated separately five times in order to improve the averaging. The concentrations of the chemical species and the coke content have been averaged over all discretization points within the network that are at the same distance from the network surface. The concentration profiles of the active centers, C_{Cp}, covered with the coke precursor, C_p, are depicted in Fig. 4. The profiles are given for different times.

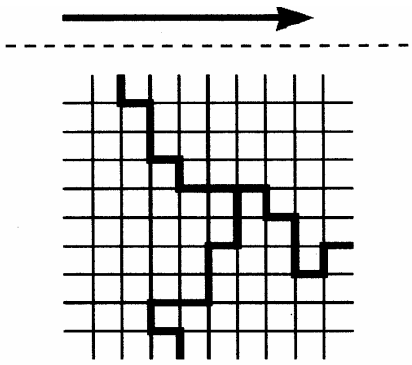

Fig. 3. Boundary conditions at the network surfaces, two-dimensional section.

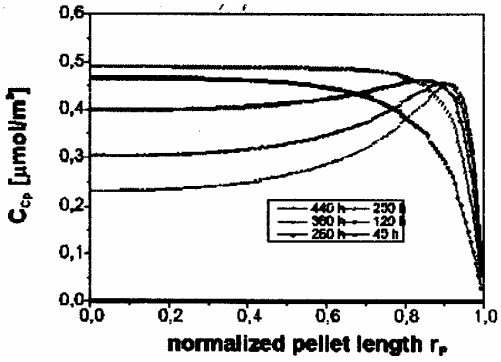

Fig. 4. Concentrations profile of the active centers covered with the coke precursor C_p for consecutive coking.

In the case of consecutive coking the maximum of the coke precursor occurs initially at the center of the network, where the concentration of the coke-forming component B is at a maximum. With increasing time, the maximum migrates towards the surface of the network.

4. Conclusions

An efficient algorithm to calculate multicomponent concentration profiles for general kinetics within three-dimensional pore networks has been developed. The algorithm is applicable to any type of a three-dimensional network and any pore shape. The pore walls may be smooth or of a fractal nature. Percolation processes can also be described by including a cluster counting algorithm. The present algorithm has been applied successfully to a complex example. It can be employed as a basic model for pore structure optimizations.

References

[1] D. Avnir, The fractal approach to heterogeneous chemistry, New York, 1989.
[2] E. A. Mason, A. P. Malinauskas, Gas Transport in porous Media: The Dusty-Gas Model; Elsevier: Amsterdam, 1983.
[3] J. W. Beeckman, G. F. Froment, Catalyst deactivation by site coverage and pore blockage, Chem. Eng. Sci., 1980, 35, 805-815.
[4] G. R. Gavalas, S. Kim, Periodic Cappillary Models of Diffusion in Porous Solids, Chem. Eng. Sci. **36**, 1111-1112 (1981).
[5] J. H. Petropoulos, J. K. Petrou, A. I. Liapis, Network Model Investigation of Gas Transport in Bidisperse Porous Adsorbents, Ing. Eng. Chem. Res. 1991, 30, 1281-1289.
[6] P. N. Sharratt, R. Mann, Some observations on the variation of tortuosity with Thiele-modulus and pore size distribution, Chem. Eng. Sci. 1987, 42, 1565-1576.
[7] S. Arbabi, M. Sahimi, Computer simulations of catalyst deactivation, Chem. Eng. Sci. **46**, 1739-1755 (1991).
[8] M. Sahimi, Transport of Macromolecules in Porous Media, J. Chem. Phys. **96**, 4718 (1992).
[9] C. McGreavy, J. S. Andrade Jr., K. Rajagopalan, Consistent Evaluation of Effective Diffusion and Reaction in Pore Networks, Chem. Eng. Sci. **47**, 2751 (1992).
[10] L. Zhang, N. A. Seaton, Prediction of the effective diffusivity in pore networks close to a percolation threshold. AIChEJ **38**, 1816-1824 (1992).
[11] F. J. Keil, C. Rieckmann, Optimization of three-dimensional catalyst pore structures. Chem. Eng. Sci. **49**, 4911-4822 (1994).
[12] N. A. Seaton, Determination of the connectivity of porous solids from nitrogen sorption measurements, Chem. Eng. Sci. **46**, 1895-1909 (1991).
[13] A. O. E. Beyne, G. F. Froment, A percolation approach for the modeling of deactivation of zeolite catalysts by coke formation, Chem. Eng. Sci. **48**, 503-511 (1993).